

Materiatronics: Modular analysis of arbitrary meta-atoms

Viktar S. Asadchy^{1,2} and Sergei A. Tretyakov¹

¹*Department of Electronics and Nanoengineering,*

Aalto University, P. O. Box 15500, FI-00076 Aalto, Finland

²*Department of General Physics, Francisk Skorina Gomel State University, 246019 Gomel, Belarus*

Within the paradigm of metamaterials and metasurfaces, electromagnetic properties of composite materials can be engineered by shaping or modulating their constituents, so-called meta-atoms. Synthesis and analysis of complex-shape meta-atoms with general polarization properties is a challenging task. In this paper, we demonstrate that the most general response can be conceptually decomposed into a set of basic, fundamental polarization phenomena, which enables immediate all-direction characterization of electromagnetic properties of arbitrary linear materials and metamaterials. The proposed platform of modular characterization (called “materiatronics”) is tested on several examples of bianisotropic and nonreciprocal meta-atoms. As a demonstration of the potential of the modular analysis, we use it to design a single-layer metasurface of vanishing thickness with record-breaking unitary circular dichroism. The analysis approach developed in this paper is supported by a ready-to-use computational code and can be further extended to meta-atoms engineered for other types of wave interactions, such as acoustics and mechanics.

I. INTRODUCTION

Metamaterials are engineered composites consisting of tailored subwavelength meta-atoms (inclusions) for controlling wave phenomena at will. During last two decades, metamaterials have attracted great interest of researchers working in different fields of physics, which resulted in important impact on fundamental science and emergence of numerous fascinating concepts [1–5]. Nevertheless, there is no universal approach for synthesis of arbitrary complex metamaterials, mainly due to the two following reasons. First, determining the required properties of single meta-atoms in the composite is a complicated inverse problem due to their mutual interactions. Second, even if such properties are known, practical realization of meta-atoms can be still very challenging because it implies rigorous design and optimization of their anisotropic properties, i.e. their entire polarizability tensors. For this reason, the vast majority of works in the literature are devoted to metamaterials whose functionality is engineered only for a specific and small number (usually single) of illumination directions. Meanwhile, properties of metamaterials excited by fields of other configurations remain unknown and unprescribed. However, this knowledge is often very important and can lead to unexpected and unique phenomena, as it was demonstrated by the example of planar chirality [6–10] which occurs only at specific oblique-angle illuminations in contrast to true three-dimensional chirality. Furthermore, in many situations, one needs to know under what excitation a meta-atom will respond in some particular way, for example, exhibiting highest possible Willis coupling [11], strongest mechanical twist [12], desired asymmetry [8, 13], or pronounced nonreciprocal properties [14]. Such arbitrary-illumination analysis, once developed, would be very beneficial for understanding and even design of bulk metamaterials and their two-dimensional counterparts (metasurfaces [15, 16]) intended to interact with waves of arbitrary nature: Acoustic, electromagnetic, mechanical, etc.

In this paper, a universal platform for analysing properties of arbitrarily complex linear meta-atoms is proposed. Although we present the results for meta-atoms designed for interactions with electromagnetic waves, the same approach can be used for the analysis of other types of wave interactions. We show that the response of a general linear meta-atom can be thought as a combination of responses of several basic modules with known, fundamental electromagnetic properties, immediately revealing the meta-atom properties for all possible excitations. Such a platform of transition from complex material units to basic elements (“materiatronics”) is in a sense analogous to electronics, where an arbitrarily complex linear circuit is represented as a network of basic elements: capacitors, inductors, resistors, and gyrators. There is also some analogy with recently introduced metatronics [17] that relies on decomposition of complex electromagnetic systems into elementary scatterers with simple dispersion properties.

The proposed modular analysis is successfully tested on several examples of dipolar meta-atoms with general electromagnetic properties, including bianisotropy and nonreciprocity. It is further demonstrated on the example of a split-ring resonator how the platform of materiatronics can be used for designing metasurfaces with maximized (or minimized) desired effects. For the convenience of the reader, the analysis approach developed in this paper is supported by a ready-to-use code and program files [18]. They provide automation in obtaining the results for a meta-atom with arbitrary customer-defined geometry.

II. MODULAR DECOMPOSITION OF POLARIZATION EFFECTS

Let us first consider an arbitrary single meta-atom located in free space so that its interaction with other meta-atoms can be neglected. Its electromagnetic response is

assumed to be linear and dipolar, which is the case for most inclusions of engineered metamaterials and meta-surfaces. No assumptions on its reciprocity or anisotropy properties are made, meaning that in the general case it can be bianisotropic and nonreciprocal. Thus, electromagnetic properties of the meta-atom are characterized by four polarizability dyadics (tensors): electric $\bar{\bar{\alpha}}_{ee}$, electromagnetic $\bar{\bar{\alpha}}_{em}$, magnetoelectric $\bar{\bar{\alpha}}_{me}$, and magnetic $\bar{\bar{\alpha}}_{mm}$, including in total 36 complex polarizability components. To apply the modular analysis of the meta-atom, one should first determine all these components. Several techniques for polarizability extraction have been proposed during the last decade [19–23] but none of them allows calculation of all the polarizability components simultaneously. In this paper, the approach based on the scattered far field probing [20] is extended [18] and utilized. It should be noted that even in the cases when the unknown meta-atom cannot be described solely by dipolar moments, the modular analysis still can be introduced using alternative T-matrix formulation which takes into account higher-order multipoles [24–26].

When the four polarizability dyadics of the meta-atom are determined, it is important to differentiate between the reciprocal and possible nonreciprocal polarization properties. Using the Onsager-Casimir symmetry relations for bianisotropic meta-atoms [27] $\bar{\bar{\alpha}}_{ee}(H_0) = \bar{\bar{\alpha}}_{ee}^T(-H_0)$, $\bar{\bar{\alpha}}_{mm}(H_0) = \bar{\bar{\alpha}}_{mm}^T(-H_0)$, $\bar{\bar{\alpha}}_{em}(H_0) = -\bar{\bar{\alpha}}_{me}^T(-H_0)$, one can represent each of $\bar{\bar{\alpha}}_{ee}$, $\bar{\bar{\alpha}}_{em}$, $\bar{\bar{\alpha}}_{me}$, and $\bar{\bar{\alpha}}_{mm}$ dyadics as a sum of the reciprocal and nonreciprocal parts (here, T is the transpose operation, H_0 denotes all external nonreciprocal parameters such as bias magnetic field or angular velocity, and $-H_0$ corresponds to the case when all these parameters switch signs). These reciprocal (subscript “r”) and nonreciprocal (subscript “n”) parts read

$$\begin{aligned} \bar{\bar{\alpha}}_{ee,r} &= \frac{\bar{\bar{\alpha}}_{ee} + \bar{\bar{\alpha}}_{ee}^T}{2}, & \bar{\bar{\alpha}}_{ee,n} &= \frac{\bar{\bar{\alpha}}_{ee} - \bar{\bar{\alpha}}_{ee}^T}{2}, \\ \bar{\bar{\alpha}}_{mm,r} &= \frac{\bar{\bar{\alpha}}_{mm} + \bar{\bar{\alpha}}_{mm}^T}{2}, & \bar{\bar{\alpha}}_{mm,n} &= \frac{\bar{\bar{\alpha}}_{mm} - \bar{\bar{\alpha}}_{mm}^T}{2}, \end{aligned} \quad (1)$$

$$\bar{\bar{\alpha}}_{em,r} = \frac{\bar{\bar{\alpha}}_{em} - \bar{\bar{\alpha}}_{me}^T}{2}, \quad \bar{\bar{\alpha}}_{em,n} = \frac{\bar{\bar{\alpha}}_{em} + \bar{\bar{\alpha}}_{me}^T}{2}. \quad (2)$$

The magnetoelectric dyadic $\bar{\bar{\alpha}}_{me}$ is excluded from Eq. (1) since it is fully determined by $\bar{\bar{\alpha}}_{em}$. It should be noticed that $\bar{\bar{\alpha}}_{ee,r}$ and $\bar{\bar{\alpha}}_{mm,r}$ dyadics are symmetric, while $\bar{\bar{\alpha}}_{ee,n}$ and $\bar{\bar{\alpha}}_{mm,n}$ are antisymmetric. However, both reciprocal and nonreciprocal electromagnetic dyadics have symmetric and antisymmetric parts.

Any symmetric dyadic (e.g., $\bar{\bar{\alpha}}_{ee,r}$) can be always represented as a linear combination of a diagonal dyadic in the initial xyz -basis and another diagonal dyadic in another basis given by complex basis vectors \mathbf{u}_1 , \mathbf{u}_2 , and \mathbf{u}_3 [28]:

$$\bar{\bar{\alpha}}_{ee,r} = \bar{\bar{I}}(\alpha_{ee}^{xx} + \alpha_{ee}^{yy} + \alpha_{ee}^{zz})/3 + \sum_i \lambda_i \mathbf{u}_i \mathbf{u}_i, \quad (3)$$

where $\bar{\bar{I}} = \mathbf{x}\mathbf{x} + \mathbf{y}\mathbf{y} + \mathbf{z}\mathbf{z}$ is the unit dyadic, $i = 1, 2, 3$; λ_i are complex coefficients such that $\sum_i \lambda_i = 0$, and notation $\mathbf{u}_i \mathbf{u}_i$ denotes a dyadic product of two vectors (the same as a dyad). The first diagonal dyadic in (3) describes isotropic electric response. The second dyadic is diagonal with zero trace in the basis of complex unit vectors. For a clear geometrical description, it is convenient to rewrite it as a linear combination of six dyadic products of real vectors in the initial basis with complex magnitudes S_j ($j = 1, 2, \dots, 6$):

$$\begin{aligned} \sum_i \lambda_i \mathbf{u}_i \mathbf{u}_i &= S_1 \mathbf{x}\mathbf{x} + S_2 \mathbf{y}\mathbf{y} + S_3 \mathbf{z}\mathbf{z} + \frac{S_4}{2} (\mathbf{x} + \mathbf{y})(\mathbf{x} + \mathbf{y}) \\ &+ \frac{S_5}{2} (\mathbf{x} + \mathbf{z})(\mathbf{x} + \mathbf{z}) + \frac{S_6}{2} (\mathbf{y} + \mathbf{z})(\mathbf{y} + \mathbf{z}). \end{aligned} \quad (4)$$

The complex amplitude coefficients S_j can be determined based on the extracted polarizability dyadics (see derivation in [18]).

Combining (3) and (4), any symmetric dyadic in the general case is decomposed into six symmetric dyads (dyadic products of real vectors), all with different complex amplitudes. Thus, the response described by any reciprocal electric dyadic $\bar{\bar{\alpha}}_{ee,r}$ is equivalent to the response of a set of six basic modules which possess only one simple polarization response: They develop electric dipole moment along a given direction when excited by electric fields along the same direction. For visualization purposes, we show these modules as straight needles, as shown in Fig. 1(a), spatially separating them for clarity. Three needles are oriented along the initial basis vectors and the other three along the bisectors of the angles between these axes. It should be noted that such decomposition is not unique and in most cases, as will be seen below, several of the modules might have negligible weights, which reduces their total number. All the needles have different complex polarization amplitudes. Hereafter, the amplitudes of the polarizability components are graphically shown as proportional to the *linear* dimension of the module and not to its volume. Now, the polarization properties of a meta-atom with $\bar{\bar{\alpha}}_{ee,r}$ given by (3) can be readily determined from Fig. 1(a). We see that, for example, an incident x -polarized plane wave will induce polarization currents and dipole moments simultaneously in three modules, resulting in polarization of the meta-atom along the x , y , and z axes (phases of polarization currents can be arbitrary). In this way, we completely describe electromagnetic properties of any meta-atom only by the types of modules, their orientations and response strength of individual modules.

Similarly, symmetric dyadic $\bar{\bar{\alpha}}_{mm,r}$ is decomposed into six dyads according to (3) and (4) (naturally, in general, with different complex amplitudes). Each decomposition term physically corresponds to a module which is reciprocal and polarizable only magnetically, only along one direction, and only by magnetic fields. For visualization purposes, we show the orientations and amplitudes of these modules by double split-ring resonators [29, 30],

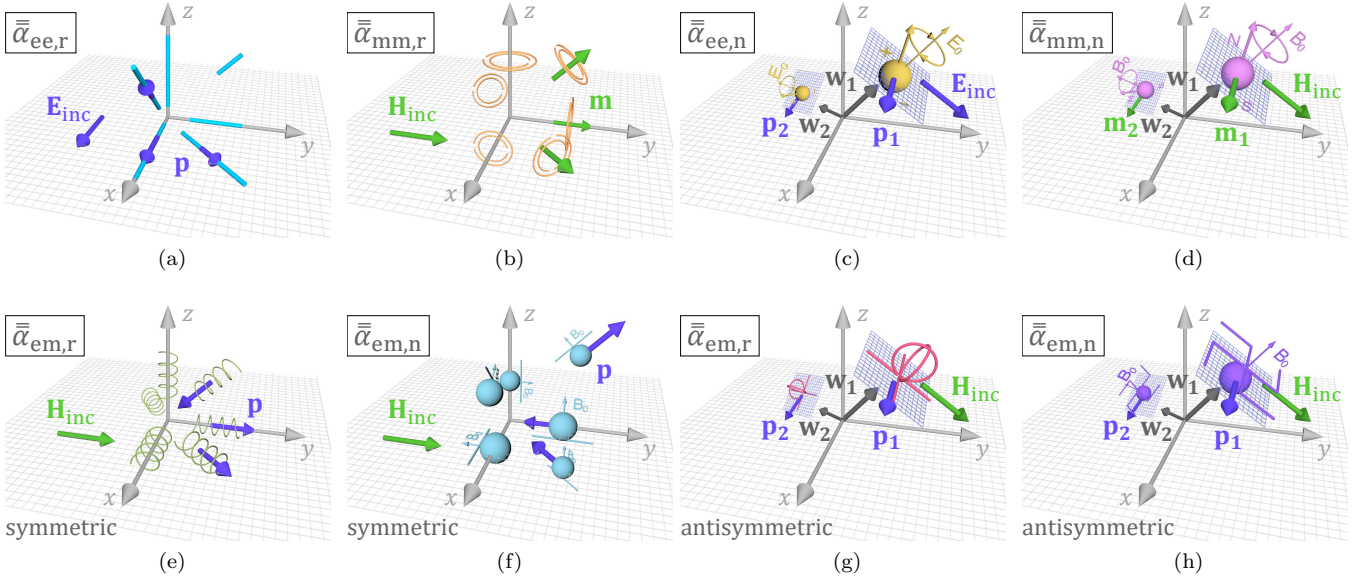


FIG. 1. Conceptual illustration of modular decomposition of different polarizability dyadics for an arbitrary dipolar meta-atom. Incident electric and magnetic fields are denoted as \mathbf{E}_{inc} and \mathbf{H}_{inc} , while \mathbf{p} and \mathbf{m} are the induced electric and magnetic dipole moments. Additional planes drawn at the antisymmetric modules are orthogonal to their symmetry axes.

because this type of polarization response is dominant for this shape (obviously, the response of such resonators is more complicated, and the modular decomposition of an actual double split-ring resonator can be found in [18]). Thus, dyadic $\bar{\alpha}_{mm,r}$ can be modelled as the combination of six different idealistic double split-ring resonators, as illustrated in Fig. 1(b).

Any antisymmetric dyadics, such as $\bar{\alpha}_{ee,n}$, can be always represented as a cross product of a complex vector and the unit dyadic (complex vector is decomposed into two real vectors with real amplitude A_1 and with imaginary amplitude jA_2) [28]:

$$\begin{aligned} \bar{\alpha}_{ee,n} = \frac{1}{2} [(\alpha_{ee}^{xy} - \alpha_{ee}^{yx})(\mathbf{x}\mathbf{y} - \mathbf{y}\mathbf{x}) + (\alpha_{ee}^{xz} - \alpha_{ee}^{zx})(\mathbf{x}\mathbf{z} - \mathbf{z}\mathbf{x}) \\ + (\alpha_{ee}^{yz} - \alpha_{ee}^{zy})(\mathbf{y}\mathbf{z} - \mathbf{z}\mathbf{y})] = A_1 \mathbf{w}_1 \times \bar{\mathbf{I}} + jA_2 \mathbf{w}_2 \times \bar{\mathbf{I}}. \end{aligned} \quad (5)$$

The unknown coefficients A_1 and A_2 and vectors \mathbf{w}_1 and \mathbf{w}_2 are calculated in [18]. The two dyadics in (5) describe two uniaxial (with one symmetry axis) modules in which polarization occurs in the direction orthogonal to the incident field and to the symmetry axis of the module. Physical interpretation of each such module in the case of nonreciprocal $\bar{\alpha}_{ee,n}$ dyadic is an electric dipole precessing in a static external electric field \mathbf{E}_0 (see Fig. 1(c)). The induced electric dipole is always perpendicular to the electric field of the incident wave. Nonreciprocal magnetic dyadic $\bar{\alpha}_{mm,n}$, likewise, is modelled by two magnetic dipoles precessing in a static magnetic field \mathbf{B}_0 (see Fig. 1(d)).

Next, one should decompose the electromagnetic dyadics $\bar{\alpha}_{em,r}$ and $\bar{\alpha}_{em,n}$ which have symmetric and antisymmetric parts and describe the bianisotropic response

of the meta-atom. The symmetric part of the former dyadic is equal to $(\bar{\alpha}_{em} + \bar{\alpha}_{em}^T - \bar{\alpha}_{me} - \bar{\alpha}_{me}^T)/4$ and according to (3) and (4) is modelled by six uniaxial chiral bianisotropic response: For visual representation, thin multi-turn metal helices (see Fig. 1(e)) are appropriate shapes to denote this fundamental polarizability effect. In general, we need two such chiral modules: Right-handed and left-handed. Incident magnetic field tangential to the helix axis generates electric polarization according to Faraday's law [31]. Likewise, the symmetric part of dyadic $\bar{\alpha}_{em,n}$, equal to $(\bar{\alpha}_{em} + \bar{\alpha}_{em}^T + \bar{\alpha}_{me} + \bar{\alpha}_{me}^T)/4$, is represented by six uniaxial nonreciprocal modules (see Fig. 1(f)). The effect of bianisotropic nonreciprocal coupling is strong in a meta-atom formed by a ferrite sphere covered by a metal wire (so-called Tellegen meta-atom) [32–34], and we use an image of this meta-atom as a notation for the presence of this fundamental block in the decomposition. An incident alternating magnetic field creates cross-polarized magnetization in the sphere (due to the off-diagonal permeability components of ferrite) which in turn results in induced electric polarization of the wire (parallel to the alternating magnetic field).

The antisymmetric part of $\bar{\alpha}_{em,r}$, expressed as $(\bar{\alpha}_{em} - \bar{\alpha}_{em}^T + \bar{\alpha}_{me} - \bar{\alpha}_{me}^T)/4$, according to (5) is modelled by two uniaxial bianisotropic asymmetric modules (one with real polarizability and another with imaginary polarizability), which we show as crossed omega-shaped wires [35], see in Fig. 1(g). Incident magnetic field orthogonal to the module axis excites mutually orthogonal electric polarization (due to Faraday's law and specific wire shape). The last part in the modular decomposition is the antisymmetric part of $\bar{\alpha}_{em,n}$ that can be calculated as

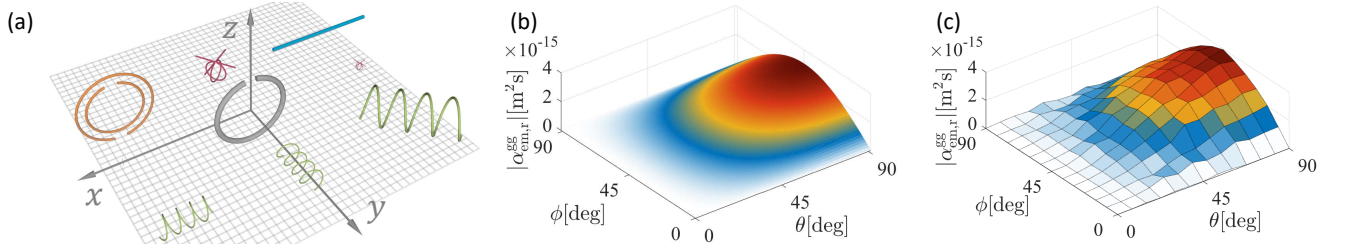


FIG. 2. (a) Modular decomposition of a split-ring resonator at its fundamental resonance. The linear dimensions of the modules are proportional to the amplitudes of the corresponding polarization effects. Surface plot illustrating the angular dependence of the amplitude of the chiral polarizability component $\alpha_{em,r}^{gg} = \mathbf{g} \cdot \bar{\alpha}_{em,r} \cdot \mathbf{g}$ of an SRR meta-atom with respect to the direction parallel to the unit vector \mathbf{g} . Results obtained from the modular decomposition (b) and results obtained using numerical full-wave simulations (c). The maximum chirality is observed when the external electric field is oriented at $\theta = 90^\circ$ and $\phi = 45^\circ$; the SRR effectively behaves as a left-handed helix oriented at these angles.

$(\bar{\alpha}_{em} - \bar{\alpha}_{em}^T - \bar{\alpha}_{me} + \bar{\alpha}_{me}^T)/4$. Two nonreciprocal modules based on ferrite sphere with swastika-shaped metal wires [36] (shown in Fig. 1(h)) can represent the required polarization properties.

III. MODULAR DECOMPOSITION FOR A SPLIT-RING RESONATOR

Next, as all the polarizability dyadics $\bar{\alpha}_{ee}$, $\bar{\alpha}_{em}$, $\bar{\alpha}_{me}$, and $\bar{\alpha}_{mm}$ are decomposed into basic modules, the universality of the materiatics platform can be demonstrated via modular analysis of realistic meta-atoms. The analysis for each of them was performed in three automated steps: Extraction of the full polarizability dyadics of the unknown meta-atom [18] (performed using a full-wave simulator [37]), decomposition of the extracted polarizability dyadics (using computational software [38]), and three-dimensional visualization of the obtained modules (using the full-wave simulator). All the supporting files for the ready-to-use automated analysis of an unknown meta-atom can be found in [18].

First, the modular analysis is applied to a split-ring resonator (SRR), as an example. The geometry and orientation of the SRR (shown in grey) in the initial basis can be seen in Fig. 2(a). The radius of the ring is 2.7 mm, the radius of the copper wire is 0.2 mm, and the gap is 0.4 mm. The decomposition was performed at the main resonance frequency of the SRR at 7.9 GHz. The power of the modular analysis is evident from Fig. 2(a) where the electromagnetic response of the meta-atom can be immediately inspected for arbitrary illuminations. The strong electric polarization response along the x -axis (straight wire) and magnetic polarization along the y -axis (magnetic module shown as a double SRR) are expected. However, additionally, the SRR exhibits perceptible omega bianisotropic response when illuminated along the z -axis [8, 13] with specific polarization of the incident wave [39]. Moreover, the decomposition includes two left-handed and one right-handed helices, indicating strong chiral properties of the SRR. Although the total chirality is zero (left- and right-handed helices precisely

compensate each other; vanishing three-dimensional chirality), for specific illumination directions one can excite predominantly left- or right-handed helices, achieving non-zero chiral effect with a planar structure (the SRR can be *infinitesimally* thin supporting only electric current). The planar chirality was observed earlier in various asymmetric structures [6–10], however, this effect remained rather weak [10, 40]. Using the modular decomposition, one can determine the chirality strength exhibited by the SRR for various orientations of the incident electric field. As it is theoretically shown in [18], the maximum chirality is achieved when the electric field is along unit vector $\mathbf{g} = \sin \theta \cos \phi \mathbf{x} + \sin \theta \sin \phi \mathbf{y} + \cos \theta \mathbf{z}$, where $\theta = 90^\circ$ and $\phi = \pm 45^\circ$ (the double sign is due to the mirror symmetry of the SRR with respect to the yz -plane). Figure 2(b) depicts theoretically calculated axial chiral polarizability of the split-ring resonator for different orientations of the incident electric field. Indeed, the maximum of chirality is observed at $\theta = 90^\circ$ and $\phi = 45^\circ$. To verify this theoretical result, polarizability $\bar{\alpha}_{em,r}$ was calculated using the above mentioned extraction technique, described separately for each orientation of the incident electric field in the range of $\theta = [0^\circ; 90^\circ]$ and $\phi = [0^\circ; 90^\circ]$ with the step of 7.5° . The results are depicted in Fig. 2(c) and are in close agreement with the theoretical ones in Fig. 2(b). The deviation in the peak amplitude value between these two figures (around 30%) can be explained by errors (which were of the order of 26% for this meta-atom) in the polarizability extraction.

As can be seen from Fig. 2(a), the SRR behaves differently for opposite illumination directions: As a left-handed helix when illuminated along the $(\mathbf{x} - \mathbf{y})$ direction (the right-handed helix in the decomposition in Fig. 2(a) is not excited) and as a right-handed helix when illuminated along the $(-\mathbf{x} - \mathbf{y})$ direction.

IV. DESIGN OF NEGLIGIBLY THIN METASURFACE WITH EXTREME CIRCULAR DICHROISM

The applicability of the modular analysis can be further demonstrated by designing a periodic metasurface of SRRs with the dimensions listed in the previous Section. The metasurface has a subwavelength square unit cell with the 10 mm side. The SRRs are *parallel* to the metasurface plane. In contrast to conventional chiral metasurfaces relying on finite thickness and three-dimensional topology with broken space-reversion symmetry, the designed metasurface exhibits strong circular dichroism (and other chiral effects) with pure two-dimensional geometry and negligible thickness. The metasurface was illuminated by circularly polarized plane waves at an angle $\phi = 45^\circ$ from the normal [$\mathbf{k}_{\text{inc}} \uparrow \uparrow (\mathbf{x} - \mathbf{y})$ in the initial basis], as shown in the inset of Fig. 3(c). For this illumination, the right-handed helix shown in Fig. 2(a) is not excited, while both left-handed helical modules are activated. Thus, the SRR behaves for this illumination as a left-handed chiral meta-atom. The plot in the

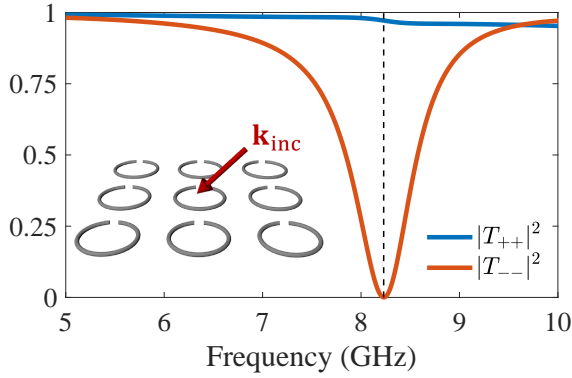


FIG. 3. Transmittance through a metasurface composed of SRRs for right (“++”) and left (“--”) circularly polarized incident waves. The inset depicts the geometry of the metasurface and wave vector \mathbf{k}_{inc} of the incidence.

figure shows frequency dispersions of the transmittance for right (“++”) and left (“--”) circular polarization of incident waves from full-wave simulations. At the resonance frequency of 8.23 GHz, the metasurface nearly fully transmits incident right circular polarization and completely reflects waves of the opposite handedness (transforming their polarization). Cross-polarization transmittance ($|T_{+-}|^2$ and $|T_{-+}|^2$) of the metasurface is indistinguishable from zero within the entire studied frequency range. Thus, circular dichroism defined as $\text{CD} = (|T_{++}|^2 + |T_{+-}|^2 - |T_{--}|^2 - |T_{-+}|^2) / (|T_{++}|^2 + |T_{+-}|^2 + |T_{--}|^2 + |T_{-+}|^2)$ is equal to 1, which is an exceptional result taking into account negligible thickness of the metasurface. Figure 4 shows CD of the designed metasurface for different illumination angles. The maximum value of CD is achieved for $\phi = 45^\circ$, while for normal incidence ($\phi = 0^\circ$) it is zero.

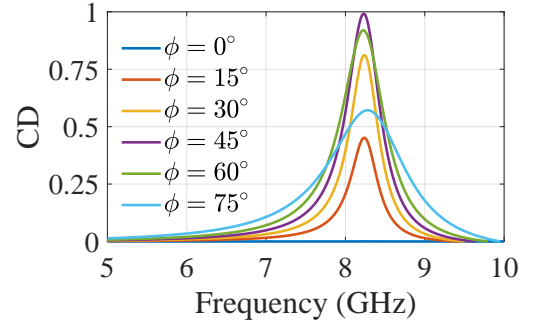


FIG. 4. Circular dichroism of the metasurface versus frequency for different illumination angles ϕ .

Such high CD significantly exceeds the values reported in the literature for planar structures to date [10, 40]. Furthermore, the effect of planar chirality achieved with the designed metasurface should be distinguished from the anisotropy effect observed in planar dielectric metasurfaces [41]. In the latter case, a metasurface exhibits symmetric response in terms of co-polarized transmission $|T_{++}| = |T_{--}|$ and asymmetry for cross-polarized transmission $|T_{+-}| \neq |T_{-+}|$.

V. MODULAR DECOMPOSITION FOR A NONRECIPROCAL VIRTUALLY MOVING META-ATOM

In this section, modular decomposition is applied to a nonreciprocal meta-atom which can be used as a constituent of metasurface-based isolators and phase shifters. The geometry of the meta-atom was adopted from [14] and is shown in Fig. 5(a). The length of the copper wire is 30 mm, and the wire radius is 0.05 mm. The ferrite sphere of 1.65 mm radius is made of yttrium iron garnet with the relative permittivity of 15, the dielectric loss tangent 10^{-4} , the saturation magnetization 1780 G, and the full resonance linewidth 0.2 Oe. The meta-atom is biased by an external $+z$ -oriented permanent magnetic field of 9626 A/m. The magnetic resonance frequency at which the modular analysis was performed is 1.975 GHz. The orientation of the magnetic bias field is along the $+x$ -direction.

As it was theoretically demonstrated in [42, Eqs. (11–12)], [43], *passive* metasurfaces operating as highly efficient nonreciprocal phase shifters or isolators at normal incidence must consist of meta-atoms which possess predominantly artificial “moving” bianisotropic coupling (i.e., the entire dyadic $\bar{\alpha}_{\text{em}}$ must be represented solely by the nonreciprocal antisymmetric part $\bar{\alpha}_{\text{em},n}$). Such result has a simple conceptual explanation. A perfect nonreciprocal isolator (lossy device) or phase shifter (lossless device) must be fully transparent from one side, meaning that they do not modify neither the amplitude nor the phase of incident waves. Such functionality may seem impossible because it implies the absence of any wave scat-

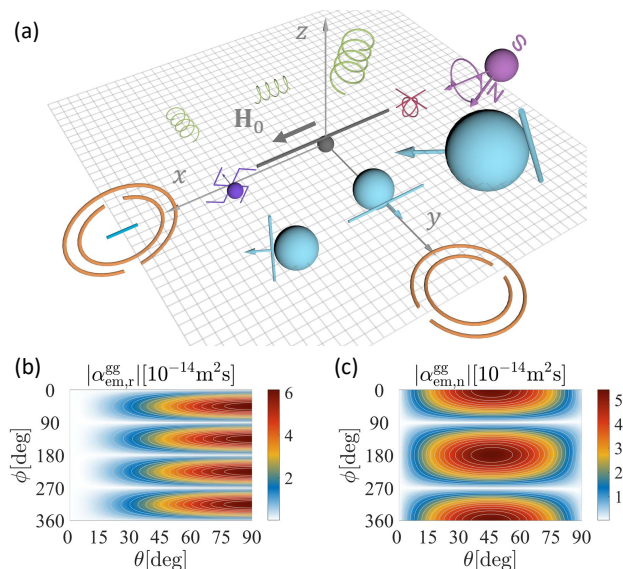


FIG. 5. (a) Modular decomposition of a nonreciprocal meta-atom (shown in grey) at its magnetic resonance frequency. Surface plots depicting axial (b) chiral and (c) Tellegen polarizabilities for different orientations of the incident electric field in the spherical coordinate system. The maximum chirality is observed when the electric field is oriented at $\theta = 90^\circ$ and $\phi = (45^\circ + 90^\circ N)$, and the maximum Tellegen properties for $\theta = 45^\circ$ and $\phi = 180^\circ N$.

tering from the metasurface, while currents in the meta-atoms are non-zero. However, in an artificial “moving” metasurface, currents induced due to bianisotropic effects and due to electric and magnetic polarizations of the meta-atoms cancel scattering from each other and form a nonscattering system. Conceptually, such metasurface resembles a thin layer with homogeneous and isotropic electric and magnetic properties moving outwards from the source of incident waves with the speed of light. This way we emulate the situation when the incident waves simply cannot reach the layer, yielding zero scattering. When illuminated from the opposite direction, the layer will strongly scatter waves.

Modular decomposition shown in Fig. 5(a) allows us to immediately understand if the nonreciprocal meta-atom under analysis in fact has necessary properties. At first glance, it seems that the meta-atom owns polarization properties of all possible kinds and, therefore, is not suitable for implementation in metasurface-based isolators. However, if one assumes the illumination of the meta-atom along the $+y$ -direction with the polarization of the incident fields given by $\mathbf{E}_{\text{inc}} = -\mathbf{x}E_{\text{inc}}$ and $\mathbf{H}_{\text{inc}} = \mathbf{z}H_{\text{inc}}$ (same assumption was made in [14]), the conclusion be-

comes opposite. From the modular decomposition, one can make the following observations. Firstly, the artificial “moving” module is excited at most since the illumination is along its axis. Secondly, the twisted omega module is not excited since the illumination is perpendicular to its axis. Thirdly, taking into account the orientation of \mathbf{E}_{inc} ($\theta = 90^\circ$ and $\phi = 180^\circ$), the chiral and Tellegen bianisotropic effects are minimized. The latter observation can be also confirmed by the plots in Figs. 5(b) and (c) depicting axial chiral and Tellegen polarizability components for different orientations of the incident electric field. The maximum of chiral response is observed for $\theta = 90^\circ$ and $\phi = (45^\circ + 90^\circ N)$ (N is an integer), while the maximum of Tellegen properties is achieved for $\theta = 45^\circ$ and $\phi = 180^\circ N$.

Thus, modular decomposition of meta-atoms is a useful method to determine their polarization properties for all illumination directions. Three other examples of meta-atom decomposition, including double-turn helix, double split-ring resonator, and nonreciprocal swastika-shaped inclusion, can be found in Supplementary Materials [18].

VI. CONCLUSIONS

The above examples clearly demonstrate the usefulness and potential of the materiatronics platform. Using relatively simple vector algebra manipulations, one can analyze the polarization properties of an arbitrary meta-atom for all possible configurations of incident plane waves, identify *all* possible (under the assumption of linear dipolar response) scattering effects in this meta-atom, and find optimal excitations for maximizing or minimizing particular effects. The proposed analysis can be exploited not only for analysis of existing meta-atoms and artificial composites based on them, but also as a starting point for meta-atom synthesis. Indeed, by tuning geometrical parameters of a meta-atom and analysing the resulting modifications of the conceptual modules in its decomposition, one can gain an insight about how to engineer necessary polarization effects. Although the modular analysis reported in this paper was introduced based on the polarizability description, it is possible to extend it analogously to susceptibility characterization, which is beneficial for metasurfaces incorporating metal-backed dielectric layers.

ACKNOWLEDGMENT

This work was supported by the Finnish Foundation for Technology Promotion and Academy of Finland (project 287894).

[1] D. R. Smith, J. B. Pendry, and M. C. K. Wiltshire. Metamaterials and negative refractive index. *Science*,

305(5685):788–792, August 2004.

- [2] A. Q. Liu, W. M. Zhu, D. P. Tsai, and N. I. Zheludev. Micromachined tunable metamaterials: a review. *Journal of Optics*, 14(11):114009, 2012.
- [3] Tie Jun Cui. Microwave metamaterials. *National Science Review*, 5(2):134–136, March 2018.
- [4] Yuri Kivshar. All-dielectric meta-optics and non-linear nanophotonics. *National Science Review*, 5(2):144–158, March 2018.
- [5] Sophia R. Sklan and Baowen Li. Thermal metamaterials: functions and prospects. *National Science Review*, 5(2):138–141, March 2018.
- [6] Charles William Bunn. *Chemical crystallography: An introduction to optical and X-ray methods*. Clarendon Press, Oxford, United Kingdom, 1961.
- [7] Richard Williams. Optical rotatory power and linear electro-optic effect in nematic liquid crystals of p-azoxyanisole. *The Journal of Chemical Physics*, 50(3):1324–1332, February 1969.
- [8] A. A. Sochava, C. R. Simovski, and S. A. Tretyakov. Chiral Effects and Eigenwaves in Bi-Anisotropic Omega Structures. In A. Priou, A. Sihvola, S. Tretyakov, and A. Vinogradov, editors, *Advances in Complex Electromagnetic Materials*, number 28 in NATO ASI Series, pages 85–102. Springer Netherlands, 1997.
- [9] A. Papakostas, A. Potts, D. M. Bagnall, S. L. Prosvirnin, H. J. Coles, and N. I. Zheludev. Optical manifestations of planar chirality. *Physical Review Letters*, 90(10):107404, March 2003.
- [10] E. Plum, X.-X. Liu, V. A. Fedotov, Y. Chen, D. P. Tsai, and N. I. Zheludev. Metamaterials: Optical activity without chirality. *Physical Review Letters*, 102(11):113902, March 2009.
- [11] Li Quan, Younes Ra’di, Dimitrios L. Sounas, and Andrea Alù. Maximum Willis coupling in acoustic scatterers. *Physical Review Letters*, 120(25):254301, June 2018.
- [12] Tobias Frenzel, Muamer Kadic, and Martin Wegener. Three-dimensional mechanical metamaterials with a twist. *Science*, 358(6366):1072–1074, November 2017.
- [13] Ricardo Marqués, Francisco Medina, and Rachid Rafi-El-Idrissi. Role of bianisotropy in negative permeability and left-handed metamaterials. *Physical Review B*, 65(14):144440, April 2002.
- [14] A. Degiron and D. R. Smith. One-way glass for microwaves using nonreciprocal metamaterials. *Physical Review E*, 89(5):053203, May 2014.
- [15] Nanfang Yu and Federico Capasso. Flat optics with designer metasurfaces. *Nature Materials*, 13(2):139–150, February 2014.
- [16] Stanislav B. Glybovski, Sergei A. Tretyakov, Pavel A. Belov, Yuri S. Kivshar, and Constantin R. Simovski. Metasurfaces: From microwaves to visible. *Physics Reports*, 634:1–72, May 2016.
- [17] Nader Engheta. Circuits with light at nanoscales: Optical nanocircuits inspired by metamaterials. *Science*, 317(5845):1698–1702, September 2007.
- [18] See Supplemental Material for additional information.
- [19] Felipe Bernal Arango and A. Femius Koenderink. Polarizability tensor retrieval for magnetic and plasmonic antenna design. *New Journal of Physics*, 15(7):073023, 2013.
- [20] Viktor S. Asadchy, Igar A. Faniayeu, Younes Ra’di, and Sergei A. Tretyakov. Determining polarizability tensors for an arbitrary small electromagnetic scatterer. *Photonics and Nanostructures - Fundamentals and Applications*, 12(4):298–304, August 2014.
- [21] Mohammad Yazdi and Nader Komjani. Polarizability calculation of arbitrary individual scatterers, scatterers in arrays, and substrated scatterers. *Journal of the Optical Society of America B*, 33(3):491–500, March 2016.
- [22] X. X. Liu, Y. Zhao, and A. Alù. Polarizability tensor retrieval for subwavelength particles of arbitrary shape. *IEEE Transactions on Antennas and Propagation*, 64(6):2301–2310, June 2016.
- [23] Theodosios D. Karamanos and Nikolaos V. Kantartzis. Full polarizability matrix extraction formulas for electrically small particles via reflection/transmission coefficients. *Progress In Electromagnetics Research*, 82:93–114, 2018.
- [24] Stefan Mühlig, Christoph Menzel, Carsten Rockstuhl, and Falk Lederer. Multipole analysis of meta-atoms. *Metamaterials*, 5(2-3):64–73, June 2011.
- [25] Martin Fruhnert, Ivan Fernandez-Corbaton, Vassilios Yannopapas, and Carsten Rockstuhl. Computing the T-matrix of a scattering object with multiple plane wave illuminations. *Beilstein Journal of Nanotechnology*, 8(1):614–626, March 2017.
- [26] Rasoul Alaei, Carsten Rockstuhl, and I. Fernandez-Corbaton. An electromagnetic multipole expansion beyond the long-wavelength approximation. *Optics Communications*, 407(Supplement C):17 – 21, 2018.
- [27] S. Tretyakov, A. Sihvola, and B. Jancewicz. Onsager-Casimir principle and the constitutive relations of bianisotropic media. *Journal of Electromagnetic Waves and Applications*, 16(4):573–587, January 2002.
- [28] Chen-To Tai. Vector and dyadic algebra. In *General Vector and Dyadic Analysis: Applied Mathematics in Field Theory*. IEEE, 1997.
- [29] B. Sauviac, C. R. Simovski, and S. A. Tretyakov. Double split-ring resonators: Analytical modeling and numerical simulations. *Electromagnetics*, 24(5):317–338, January 2004.
- [30] J. D. Baena, J. Bonache, F. Martin, R. M. Sillero, F. Falcone, T. Lopetegui, M. A. G. Laso, J. Garcia-Garcia, I. Gil, M. F. Portillo, and M. Sorolla. Equivalent-circuit models for split-ring resonators and complementary split-ring resonators coupled to planar transmission lines. *IEEE Transactions on Microwave Theory and Techniques*, 53(4):1451–1461, April 2005.
- [31] Viktor S. Asadchy, Ana Díaz-Rubio, and Sergei A. Tretyakov. Bianisotropic metasurfaces: physics and applications. *Nanophotonics*, 7(6):1069–1094, 2018.
- [32] Bernard DH Tellegen. The gyrator, a new electric network element. *Philips Research Reports*, 3(2):81–101, 1948.
- [33] E. O. Kamenetskii. On the technology of making chiral and bianisotropic waveguides for microwave propagation. *Microwave and Optical Technology Letters*, 11(2):103–107, February 1996.
- [34] S. A. Tretyakov, S. I. Maslovski, I. S. Nefedov, A. J. Vititanen, P. A. Belov, and A. Sanmartin. Artificial Tellegen particle. *Electromagnetics*, 23(8):665–680, January 2003.
- [35] Mamdouh M. I. Saadoun and Nader Engheta. A reciprocal phase shifter using novel pseudo-chiral or Ω medium. *Microwave and Optical Technology Letters*, 5(4):184–188, 1992.
- [36] Sergei A. Tretyakov. Nonreciprocal composite with the material relations of the transparent absorbing boundary. *Microwave and Optical Technology Letters*, 19(5):365–

- 368, December 1998.
- [37] *ANSYS Electronics Desktop 2017.2: www.ansys.com.*
 - [38] *MATLAB and Statistics Toolbox Release 2018a, The MathWorks, Inc., Natick, Massachusetts, USA.*
 - [39] Linear scale of the antisymmetric modules (such as the twisted omega module) represents the strength of the polarization response to unpolarized incident waves propagating along the module's axis.
 - [40] Ranjan Singh, Eric Plum, Weili Zhang, and Nikolay I. Zheludev. Highly tunable optical activity in planar achiral terahertz metamaterials. *Opt. Express*, 18(13):13425–13430, Jun 2010.
 - [41] Chihhui Wu, Nihal Arju, Glen Kelp, Jonathan A. Fan, Jason Dominguez, Edward Gonzales, Emanuel Tutuc, Igal Brener, and Gennady Shvets. Spectrally selective chiral silicon metasurfaces based on infrared Fano resonances. *Nature Communications*, 5:3892, May 2014.
 - [42] Y. Ra'di, V. S. Asadchy, and S. A. Tretyakov. One-way transparent sheets. *Physical Review B*, 89(7):075109, February 2014.
 - [43] S. Taravati, B. A. Khan, S. Gupta, K. Achouri, and C. Caloz. Nonreciprocal nongyrotropic magnetless metasurface. *IEEE Transactions on Antennas and Propagation*, 65(7):3589–3597, July 2017.